

Thin Network Extraction in 3D Images: Application to Medical Angiograms

Veronique PRINET Olivier MONGA

Ge CONG Xie Sheng LOA* SongDe MA**

Institut National de Recherche en Informatique et Automatique
Domaine de Voluceau, BP 105 - 78153 Le Chesnay CEDEX, France.

* National Laboratory of Pattern Recognition
Institute of Automation - Chinese Academy of Sciences
P0 Box 2728, Beijing 100080, China.

Veronique.Prinet@inria.fr

<http://www-rocq.inria.fr/syntim/research/prinet>

Abstract

Thin network extraction from three dimensional images is a new issue in computer vision. It is of major importance in medical vascular imaging for diagnostic, therapy planning and surgery. In this paper, we develop a framework for automatic thin network extraction from the volumic image. The approach consists in treating the 3D image as a hyper-surface of \mathbb{R}^4 . It is shown that the crest points of this hyper-surface correspond to the center line of the thin network in the image. Using a simple mathematical model, we establish the relationship between the computed principal curvatures of the hyper-surface and the geometry of the network. Promising results are shown on synthetic and real vascular images.

Key words: thin network, differential geometry, differential characteristics, principal curvatures, hyper surface, crest point, feature detection, medical image, angiogram.

1 Introduction

The extraction of thin networks in three dimensional (3D) images is a new issue in computer vision. Thin networks detection has been abundantly treated in bidimensional (2D) images –for roads detection in satellite images, for example–, but few works have been done in 3D. The need is however of major importance, in particular in medical imaging, i.e. in vascular imaging.

The modern 3D medical imaging technologies (Spiral Computer Tomographic Scanner, Magnetic Resonance Angiograms) provide vascular images with very high accuracy. In these angiograms, voxels representing the vessels have higher or lower intensity level than the other tissues. Clinical routine viewing is based on 2D slices or Maximal Intensity Projection (M.I.P.) images of the 3D data. However this views are not satisfying because the notion of spacial localization in the volume is lost. Therefore, to be able to represent the vascular tree as a volume in a three dimensional space, it is required to extract the vascular network from the image, and then to visualize it independently of the other anatomical structures present in the image.

In this paper, we develop a method for thin network extraction in 3D images. For this purpose, we make use of the differential geometry of surfaces.

Recently, it has been shown that the characteristic features of an n D image can be retrieved by computing the geometrical invariants of the surface in \mathbb{R}^{n+1} traced by $(x_1, \dots, x_n, I(x_1, \dots, x_n))$. This approach has been successfully used for network extraction from 2D medical and satellite images [14, 7]. It has also been applied to 3D images in order to retrieve the characteristic lines on the surface of a 3D object [12]. In this case, the 3D non-isosurface is treated as a hyper-surface in the four dimensional (4D) space.

We pursued these works and developed the following aspects:

- We show that the whole volumic image can be treated as a hyper-surface of \mathbb{R}^4 . We compute the second and third order differential characteristics of this surface, i.e. the three principal curvatures, the three principal directions, and the extrema of the maximum curvature. We show that the crest points of the hyper-surface correspond to the center line of the thin network of the image.

- Using a simple mathematical model of the vessel, we set up the relationship between the three principal curvatures and the geometry of the vessel.

Unlike methods proposed by others [18, 10], this approach has two major interests: first, no *a priori* knowledge on the shape of the network or its spacial localisation is required; and moreover, it is entirely automatic, without the need of the intervention of the user.

The paper is organized as follows:

We give in section 2 a short bibliographic review; in section 3 we recall the principal results and conclusions given by Monga & Benayoun concerning the differential geometry in \mathbb{R}^4 ; we develop in section 4 the method for crest points extraction (defined as the local maxima of the maximum curvature) on the hyper-surface traced by the image; using a simple mathematical model, we establish the relationship between the three principal curvatures computed on the hyper-surface and the shape of the vessel; section 5 presents the results on synthetic images and on a real angiography. We conclude in section 6.

2 Related Works

The extraction of thin networks began in the bidimensional images with the problematic of automatic detection of roads in satellite images. Recently, Jedynak developed a probabilistic approach of the problem [8]. He uses the *Jeu des vingt questions* (or, *Game of 20 questions*) in order to track the road in the image. This method give interesting results but still requires the intervention of the human to give starting points to the algorithm.

It has been proposed a method using the differential geometry of surfaces to extract roads from small satellite images [7]. It is shown that the center line of the road corresponds to the crest-line of the parametric surface associated with the image. This method enables the detection of the roads in the image, but does not get rid of false-detections.

The same approach has been successfully used for blood vessels detection in 2D medical images [14]. In this case, the thin vessels are considered as the thin networks. Some post-processing has been applied to eliminate remaining noise.

Satellite images and medical images, how much different they can be, have the commun

point to be very noisy : the structure to be extracted (road or vessel) is surrounded by many other structures, it cannot always be well distinguished from the background, it is not consistent in the whole image (change of intensity level and shape).

In the 3D images, the same difficulties appear. The only works known on thin network extraction in 3D are on medical images. Verdonck [18] proposes a technique based on a *a priori* model of the vessel. However, the vessels still cannot be detected automatically and the human intervention is required. Another approach uses the mathematical morphology in order to characterize the vessels shape [10].

These two previous methods, have the main inconvenience to ask for some *a priori* knowledge of the vessels shape. This will be an important limitation when dealing with special cases, i.e, pathological cases, which, of course, are major cases for the physicians.

In an other hand, the extraction of typical features from 3D images has been treated by many authors. Among them, Feldmar extracted features from 3D and 2D images of the same object in order to establish the correspondence between the two images [5]. Thirion extracts feature points based on geometrical invariants from a 3D surface, for registration. More recently, it has been developed the idea of differential characteristics in \mathbb{R}^4 [15, 12]. The 3D image is thus treated as a hyper-surface of the four dimensional space. The geometrical invariants of the volumetric image can be retrieved by computing the differential characteristics of the hyper surface [12].

This last work was limited to the 3D contours of the volumic image. We will show in the next sections, that, by applying the same approach to the whole volumetric image, we can extract typical geometrical features of the 3D image, in particular the thin networks.

3 Differential Geometry in \mathbb{R}^4

A good introduction to differential geometry can be found in Docarmo [4] or Koenderink [9]. Here, we suppose the lectors familiar with the notions of differential geometry of surfaces,

such as the first and second fundamental forms, principal curvatures and directions. In this section, we recall the main conclusions given in [12], concerning the differential geometry of surfaces in the four dimensional space.

Parametrized surface :

Let be $I(x, y, z)$, the grey level function of a 3D image. M is an application from an upset $U \subset \mathbb{R}^3$ to E defined such as:

$$M : \mathbb{R}^3 \rightarrow E$$

$$(x, y, z) \rightarrow (x, y, z, I(x, y, z))$$

$M(U)$ forms the parametrical surface described by:

$$\Sigma = \left\{ \vec{v} \in \mathbb{R}^4 / \vec{v} = (x, y, z, I(u, v, w)) \right\} \quad \text{where } u = x, v = y, w = z.$$

Thus, the point P_0 with coordinates (x_0, y_0, z_0) in \mathbb{R}^3 corresponds to $M_0 : (x_0, y_0, z_0, I_0)$ in \mathbb{R}^4 . The plan formed by the vectors $\vec{M}_u, \vec{M}_v, \vec{M}_w$:

$$\vec{M}_u = \frac{\delta \vec{M}}{\delta u} \Big|_{M_0} = (1, 0, 0, I_x(x_0, y_0, z_0))^t$$

$$\vec{M}_v = \frac{\delta \vec{M}}{\delta v} \Big|_{M_0} = (0, 1, 0, I_y(x_0, y_0, z_0))^t$$

$$\vec{M}_w = \frac{\delta \vec{M}}{\delta w} \Big|_{M_0} = (0, 0, 1, I_z(x_0, y_0, z_0))^t$$

is tangent to the surface at M_0 . I_x, I_y, I_z are the partial derivatives of the image along the directions x, y and z respectively. The normal of the hyper-surface \vec{N}_0 is given by: $\vec{N}_0 = \frac{1}{\sqrt{D}} (\vec{M}_u \wedge \vec{M}_v \wedge \vec{M}_w)$, with $D = 1 + I_x^2 + I_y^2 + I_z^2$.

Fundamental forms and the Weingarten Matrix :

As in the 3D space, the first and second fundamental forms, Φ_1 and Φ_2 respectively, are defined in the tangent plan of the surface. It has been shown that they are functions of the partial derivatives of the image up to order two:

$$\Phi_1 = \begin{pmatrix} 1 + I_x^2 & I_x I_y & I_x I_z \\ I_x I_y & 1 + I_y^2 & I_y I_z \\ I_x I_z & I_y I_z & 1 + I_z^2 \end{pmatrix} \quad \Phi_2 = \frac{1}{\sqrt{D}} \begin{pmatrix} -I_{xx} & -I_{xy} & -I_{xz} \\ -I_{xy} & -I_{yy} & -I_{yz} \\ -I_{xz} & -I_{yz} & -I_{zz} \end{pmatrix} \quad (1)$$

The Weingarten Matrix W is thus defined by:

$$W = \Phi_1^{-1}\Phi_2 = \begin{pmatrix} a & b & c \\ d & e & f \\ g & h & i \end{pmatrix} \quad (2)$$

Note that the Weingarten matrix is not necessary symmetric unless the basis $\{\vec{M}_u, \vec{M}_v, \vec{M}_w\}$ is an orthonormal basis.

Principal curvatures and directions :

In \mathbb{R}^3 , a surface is described by its maximal and minimal curvatures. However, in \mathbb{R}^4 , the hyper-surface has three principal curvatures: the *maximum, medium, and minimum curvatures*. The maximum curvature is the curvature whose amplitude is maximal, the minimum curvature is the one whose amplitude is minimal and the medium curvature is the remaining one. The *maximum, minimum and medium directions* are the associated directions.

The principal curvatures of the hyper-surface correspond to the eigenvalues of the Weingarten matrix, and the principal directions are the eigenvectors [15, 12]. It has been pointed out that the maximum curvature is the most reliable to extract characteristic features. However, if in \mathbb{R}^3 the geometrical meaning of the two principal curvatures is clear, to understand in \mathbb{R}^4 what represents these three curvatures is not obvious .

This method has recently been applied to characterize the geometry of 3D contours. We extend the approach to extract characteristic points from the whole volumetric image.

4 Thin Networks Detection

In this section, we will first detail the method to extract typical features from the volumetric image by computing the second and third order differential characteristics of the hyper-surface. Then, we establish the relationship between the principal curvatures and the geometry of the network .

4.1 2^{nd} and 3^{rd} order differential characteristics extraction

The principal curvatures are retrieved by solving the characteristic equation of the Weingarten matrix W given by:

$$\lambda_i^3 - 3H\lambda_i^2 + P\lambda_i - G = 0 \quad i = \{1, 2, 3\} \quad (3)$$

where, using equation (2):

$$\begin{aligned} H &= \lambda_1 + \lambda_2 + \lambda_3 &= \frac{a + e + i}{3} \\ P &= \lambda_1\lambda_2 + \lambda_1\lambda_3 + \lambda_2\lambda_3 &= ae + ai + ei - fh - bd - cg \\ G &= \lambda_1\lambda_2\lambda_3 &= \det(W) \end{aligned} \quad (4)$$

Thus, the maximum, minimum and medium curvatures are respectively $c_1 = \max(|\lambda_1|, |\lambda_2|, |\lambda_3|)$, $c_3 = \min(|\lambda_1|, |\lambda_2|, |\lambda_3|)$, $c_2 = med(|\lambda_1|, |\lambda_2|, |\lambda_3|)$. The points where of $\lambda_1 = \lambda_2 = \lambda_3$, are defined as umbilic points.

The principal associated directions, $\vec{d}_1, \vec{d}_2, \vec{d}_3$, verify the following equation:

$$W \vec{d}_i = \lambda_i \vec{d}_i \quad i = \{1, 2, 3\} \quad (5)$$

In the basis of the tangent plan, the principal directions $\vec{d}_i = (d_{ui}, d_{vi}, d_{wi})$, can be written using equations (2) and (5):

$$\vec{d}_i = \begin{pmatrix} (e - \lambda_i)(i - \lambda_i) - fh \\ hg - a(i - \lambda_i) \\ ah - g(e - \lambda_i) \end{pmatrix} \quad (6)$$

The three principal directions are orthogonal to each other and belong to the tangent plan at the surface on each point. To retrieve their coordinates in the $(0, x, y, z, t)$ basis we only do a change of basis using the Jordan Matrix $J = (\vec{M}_u, \vec{M}_v, \vec{M}_w)$. Thus we obtain: $\vec{d}_i = JI = (d_{ui}, d_{vi}, d_{wi}, (I_x d_{ui} + I_y d_{vi} + I_z d_{wi}))^t$.

Extrema of curvature :

The extraction of the extrema of curvatures consists in finding the points where the maximum curvature is locally maximal. These points are called *crest points*. Crest points have

been previously defined as the zero crossings of the directional derivative, thus requiring the computation of the third order partial derivatives. For simplicity, we only extracted the crest points by a simple comparison procedure. Thus we define:

A point $P = (x, y, z)$ of the image, is a **crest point** if the absolute maximum curvature at P is higher than at P_a and P_b , where $P_a = \begin{pmatrix} x + d_x \\ y + d_y \\ z + d_z \end{pmatrix}$ and $P_b = \begin{pmatrix} x - d_x \\ y - d_y \\ z - d_z \end{pmatrix}$, and $\vec{d}_1 = (d_x, d_y, d_z)^t$ is the maximal normalized direction computed at (x, y, z) .

Note that this definition mentions that the crest points are retrieved in the space of the image. In order to proceed to the crest points extraction, we approximate the maximum direction computed in \mathbb{R}^4 — $\vec{d}_1 = (d_u, d_v, d_w, d_t)^t$ resulting from equation (6)— by its projection into \mathbb{R}^3 : $\vec{d}_1 = (d_x, d_y, d_z)^t$. Such an approximation is only valid if the fourth component d_t is null, which is reasonably true at the crest points (but it false elsewhere).

Furthermore, because P_a and P_b do not necessarily correspond to the center of a pixel, we compute the curvatures at those points by a linear interpolation from the eight neighbors. We consider that P_a and P_b are located at a unit distance from P .

In summary, the procedure is as follows:

1. Compute the partial derivatives of the image in x and y up to order two,
2. Compute the principal curvatures and directions at each voxel on the image, from equations (2), (3) and (6),
3. For each voxel P (with maximum curvature and direction, c_1 and \vec{d}_1 respectively):
 - Compute the maximum curvatures at P_a and P_b , called c_1^a and c_1^b ,
 - Retain P as a crest point if: $|c_1^a| \leq |c_1|$ & $|c_1^b| \leq |c_1|$

4.2 Geometrical Meaning of the three Principal Curvatures

In order to well understand the meaning of the three principal curvatures, we propose in this section to study a simple mathematical model: the cylinder, inside which the intensity level is given by a function $I(x, y, z)$. The cylinder is an appropriate model in the sense that it could be associated, at least locally, to the shape of the vessel [17].

Consider the model given by:

$$I(x, y, z) = \sqrt{R^2 - (y - y_0)^2 - (z - z_0)^2} \quad (7)$$

$$(y - y_0)^2 + (z - z_0)^2 < R^2 \quad \|(x - x_0)\| < l \quad (8)$$

This is a $2l$ long cylinder, with radius R , and with its main axis along the x axis. The intensity level is maximal on the central axis and null at the borders. Because the intensity level is constant along the x axis, we will see that we can treat this $3D$ model like a $2D$ case.

From equations (1) and (2), and by considering the partial derivatives in x are equal to zero, we can write the Weingarten matrix such as:

$$W = \begin{pmatrix} 0 & 0 & 0 \\ 0 & I_y I_z I_{yz} - I_{yy}(1 + I_z^2) & I_y I_z I_{yy} - I_{yz}(1 + I_y^2) \\ 0 & I_y I_z I_{zz} - I_{yz}(1 + I_z^2) & I_y I_z I_{yz} - I_{zz}(1 + I_y^2) \end{pmatrix} \quad (9)$$

The coefficients of the characteristic equation, H , P and G defined at equation (3) are now:

$$H = \frac{1}{3} \frac{(2I_y I_z I_{yz} - I_{yy}(1 + I_z^2) - I_{zz}(1 + I_y^2))}{(1 + I_y^2 + I_z^2)^{3/2}}$$

$$P = \frac{I_{yy} I_{zz} - I_{yz}^2}{(1 + I_y^2 + I_z^2)^2} \quad G = 0$$

We pose $\tilde{H} = \frac{3}{2}H$. Then the equation characteristic can be re-written:

$$\begin{cases} \lambda^2 - 2\tilde{H}\lambda + P = 0 \\ \lambda_0 = 0, \quad \tilde{H} = \frac{3}{2}H \end{cases}$$

The resolution of (3) is then reduced to solve a second order equation which roots, λ_1 and λ_2 verify:

$$\lambda_1 = \tilde{H} + \sqrt{P - \tilde{H}^2} \quad \lambda_2 = \tilde{H} - \sqrt{P - \tilde{H}^2}$$

which is exactly similar to a two dimensional case, in the $(0, y, z)$ plan.

If we consider the distribution intensity $I = \sqrt{R^2 - (y - y_0)^2 - (z - z_0)^2}$ inside the cylinder, one can notice that the imaginary surface given by $(y, z, I(y, z))$ would describe a sphere. By computing the partial derivatives and then after H and P , we can easily show that both λ_1 and λ_2 take at any point the value of $\frac{1}{R}$, that is, the curvature of the sphere of radius R .

Thus, from the model described in (7), we obtain three curvatures: $c_3 = 0, c_1 = c_2 = 1/R$. Because of the choice of the intensity distribution I , the curvatures c_1 and c_2 computed in \mathbb{R}^4 are constant all over the cylinder, from the contour to the central axe. More over they are exactly inversly proportional to the radius of the cylinder.

If we now consider the model given by:

$$I(x, y, z) = \sqrt{1 - \left(\frac{y - y_0}{b}\right)^2 - \left(\frac{z - z_0}{c}\right)^2}$$

$$\left(\frac{y - y_0}{b}\right)^2 + \left(\frac{z - z_0}{c}\right)^2 < 1 \quad \|(x - x_0)\| < l \quad (10)$$

Once again, the derivative along the x axis will be null. By the same reasoning, we could retrieve the formulation of the two non-null principal curvatures, c_1 and c_2 , and show that they correspond to the description of the ellipsoide; c_3 will be equal to zero at any point. c_1 and c_2 will be maximal on the cylinder's axe and inversly proportional to b and c . Therefore, the three curvatures will describe exactly the shape of the object.

These two examples are particular and ideal cases. However, we were able to show that the three principal curvatures of the hyper-surface of \mathbb{R}^4 , are characteristic of the geometry of the cylindric model. We reduced the resolution of a three order equation to a second order problem, because the intensity variation along one of the axis of the Cartesien space $(0x)$ was null. Therefore, the two principal directions which curvatures are not null, \vec{t}_1 and \vec{t}_2 , belong to the plan $(0yz)$, independtly of x . Thereafter, \vec{t}_1 and \vec{t}_2 transposed in \mathbb{R}^4 are linear functions of $\frac{\delta M}{\delta v}$ and $\frac{\delta M}{\delta w}$, and are independent of $\frac{\delta M}{\delta u}$.

In real data, if we assume that the vessel can be locally associated to a cylinder of length $l < \varepsilon$, the principal curvatures will give us an estimation of the vessel width. However, in

particular because the intensity distribution inside the vessel is unknown, we cannot ensure that the values of the principal curvatures will correspond to the exact dimensions of the vessel.

5 Results

We applied the method to synthetic images representing thin structures of simple geometrical form. We also show the first results on real Magnetic Resonance Angiography (M.R.A.).

5.1 Synthetic images

The images at the left of figure 1 represent the synthetic models, respectively, a propeller, a rectangle, both in filament, and a cylinder. The filament width is of one voxel. The cylinder diameter is three voxels; the intensity distribution inside the cylinder is given by : $I = \exp(-r^2)$, $r = (y - y_0)^2 + (z - z_0)^2 \forall x$, where (x_0, y_0, z_0) is the center of the image.

The images on the right illustrate the results of the crest point extraction with the hypersurface method. Only the crest points which maximal curvature is positive and higher than a given threshold are retained. In the case of the square, the object is totally recovered. In the case of the propeller, the difference between the original image and the crest lines extracted, shows an error of recovery of 0.006 percent. For the cylinder, the crest line extracted correspond exactly to its axis.

We note therefore that the method enable to detect the thin structures, how thin the structure is.

5.2 Medical images

The figure 2, on top, represents different successive slices of a cerebral Magnetic Resonance Angiography. The vessels have higher intensity than the other structures. The resolution of the image is $1mm^3$, and its dimensions are: $64*180*230$ voxels. The vessels width varies between one and four voxels.

At bottom, are the results of the crest points extraction, under the form of a projection of the 3D data along the y and z axes. A threshold on the maximal curvature has been previously applied. We note the good continuity of the extracted points. However, only the largest vessels have been retrieved. The thresholding leads to the lost of the thinnest vessels at the periphery.

6 Conclusion

By combining different previous works [12, 14], we were able to use the differential geometry of surface for the purpose of 3D network extraction. It has been shown that there is a direct relationship between the differential characteristics computed on the hyper-surface traced by the image and the geometry of the thin network in the image it self. Results on synthetic and reel data show the interest of the method: the thin network is exactly detected, even if it is one pixel large. However to get rid of the thresholding which leads to the lost of the smallest vessels, it is required to applied some advanced post-processing. We illustrate at figure 3, the solution already proposed in a 2D angiogram of the coronaries: chaining the crest points into crest lines. We are now working on a 3D chaining algorithm.

References

- [1] H. Asada and M Brady, *The curvature primal sketch*, IEEE transactions on pattern analysis and machine intelligence, vol 1 , January 1986.
- [2] R. Deriche, *Recursively implementing the gaussian and its derivatives*, Research report - INRIA, Mai 1993.
- [3] R. Deriche and Gerard Giraudon, *A computational Approach for Corner and Vertex Detection*, International Journal of Computer Vision, 1993.
- [4] M. P. Do Carmo, *Differential geometry of curves and surfaces*, Pentice Hall, 1976.
- [5] J. Feldmar, N. Ayache anf F. Betting, *3D-2D projective transformation of free curves and surfaces*, Research report - INRIA, December 1994.
- [6] G. Giraudon and R. Deriche, *On corner and vertex detection*, Conference on Computer Vision and Pattern Recognition, June 1991.

- [7] R. Horaud and O. Monga, *Vision par ordinateur: outils fondamentaux*, Edition Hermes, 1995.
- [8] B.Jedynak and J.P. Roze, *Tracking roads in SPOT images by playing twenty questions*, International Workshop on Automated Extraction of Man-Made Object from Aerial and Space Imagery, April 1995.
- [9] J.J. Koenderink, *Solid shapes*, The MIT Press, 1990.
- [10] Y. Masutani, T. Kurihara and M. Suzuki and T. Dohi, *Quantitative vascular shape analysis for 3D MR-Angiography using mathematical morphology*, Conference on Computer Vision, Virtual Reality, and Robotics in Medicine, 1995 April.
- [11] O. Monga, R. Lengagne and R. Deriche, *Extraction of the zero-crossing of the curvature in volumic 3D medical images: a multi-scale approach*, IEEE Conference in computer vision and pattern recognition, 1994.
- [12] O. Monga and S. Benayoun, *Using partial derivatives of 3D images to extract typical features*, CVGIP: Image understanding, Mars 1995.
- [13] J. Ponce and M. Brady, *Toward a surface primal sketch*, 1985 IJCAI.
- [14] V. Prinet and O. Monga, *Crest-lines for Vessels detection in angiograms*, Second Asian Conference on Computer Vision, Singapore, December 1995.
- [15] B.H. Romeny, L. Florack, A. Salden, and M. Viergever, *Higher order differential structure of images*, In H.H. Barrett and A.F. Gmitro editors, Information Processing in Medical Imaging, pages 77-93, Flagstaff Arizona (USA), June 1993, IPMI'93, Springer-Verlag.
- [16] P.T. Sander and S.T. Zucker, *Singularities of Principal Direction Fields from 3D Images*, IEEE transactions on pattern analysis and machine intelligence, vol 14 , no 3 March, 1992.
- [17] U. Shani and D.H. Ballard, *Splines as embeddings for generalized cylinder*, Computer Vision Graphics and Image Processing, vol 27, 1984.
- [18] B. Verdonck, I. Bloch, H. Maitre, *Blood Vessels Segmentation and Visualization in 3D MR and Spiral CT Angiography* CAR, 1995.

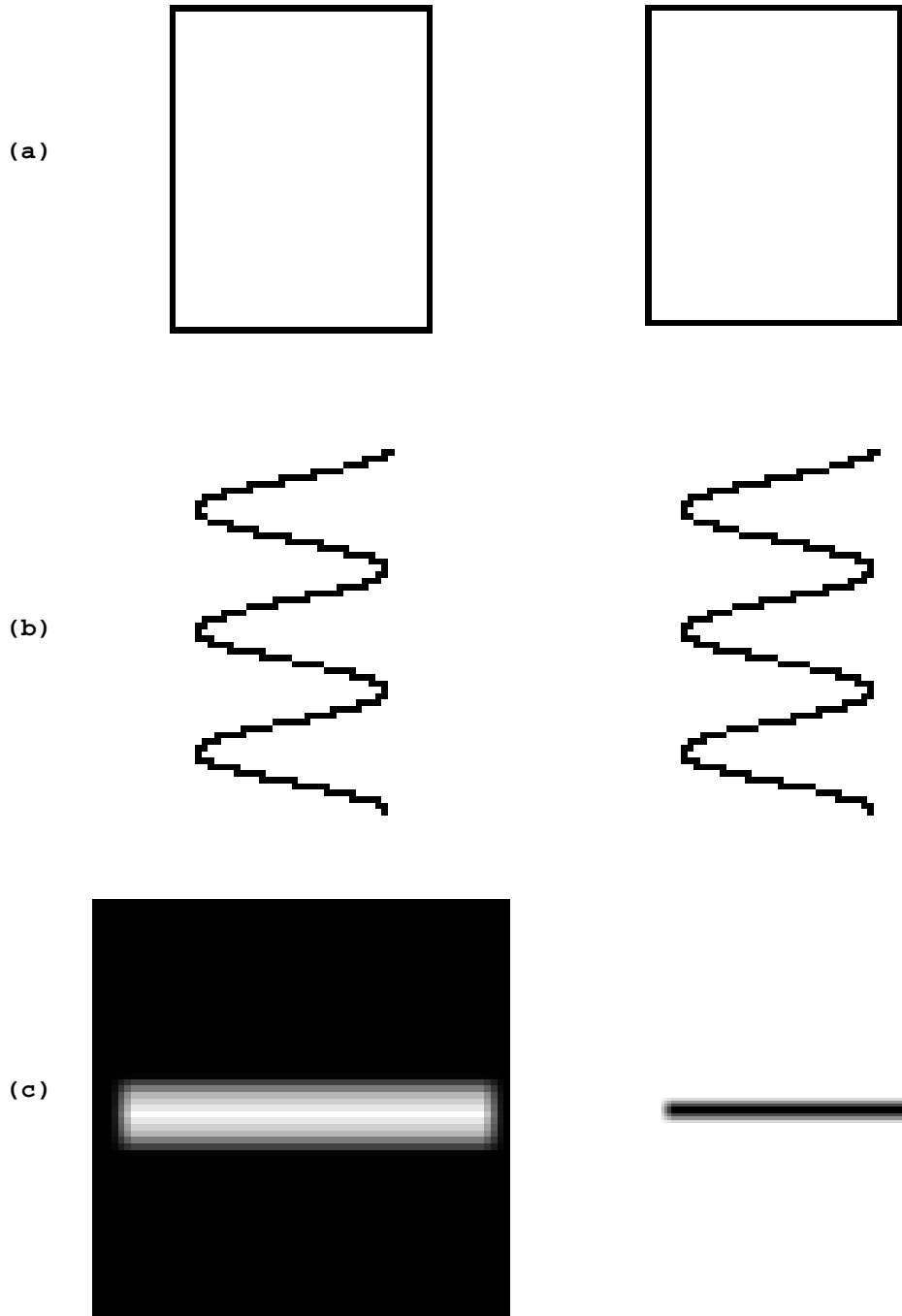
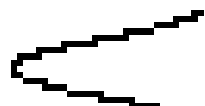


Figure 1: Left: 3D synthetic model: a square (a) and a propeller (b) in filament, a cylinder (c) ; Right: projective view of the crest points extracted from the corresponding 3D model.



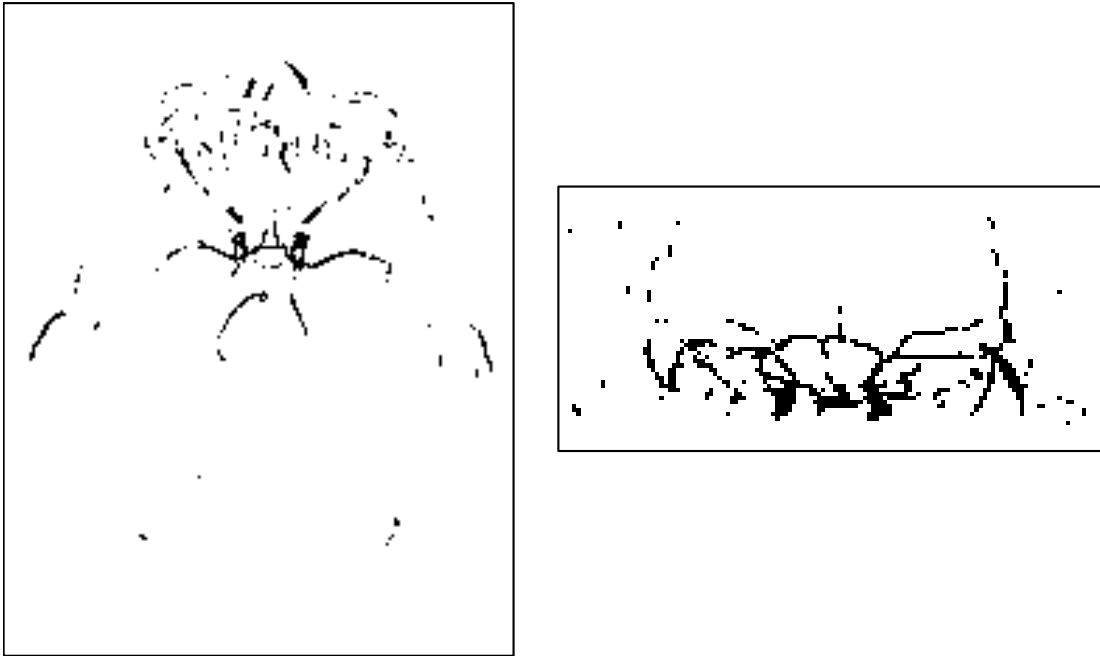
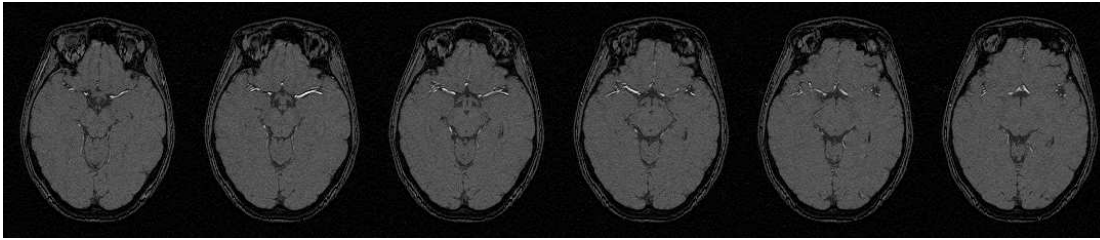


Figure 2: top slices of the 3D original MRA;
 bottom: two perspective views of the 3D crest points.

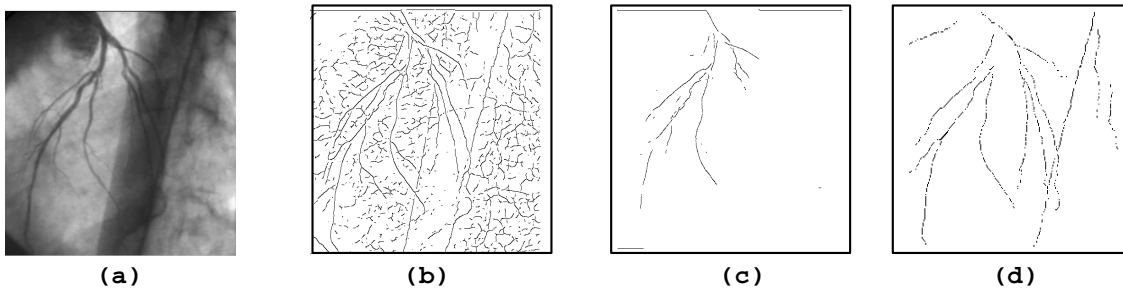


Figure 3: (a) original coronarography; (b) result of the crest points extraction; (c) after thresholding image b on the maximal curvatures; (d) after chaining the crest points from image b into crest lines.